Spatial variation in Mount St. Helens clones from coda wave analysis

Roel Snieder[1], Stephanie Prejean[2], and Jeff Johnson[3]

[1] *Center for Wave Phenomena and Dept. of Geophysics, Colorado School of Mines, Golden CO 80401*
[2] *USGS Alaska Volcano Observatory, 4200 University Ave., Anchorage, AK 99508*
[3] *Department of Earth Sciences, University of New Hampshire, Durham, NH 03824*

ABSTRACT
Volcanic activity in Mount St. Helens in 2004 was accompanied by highly similar seismic events. The coda of recorded waveforms slowly changes on a time-scale of a day. We analyze these changes using coda wave interferometry. The absence of a systemic phase shift rules out a velocity change. A comparison of the changes in the waveforms in different time windows rules out a change in the source-time function. We show that the changes in the coda waves can be explained by a change in the source position of about 100 m/day. This estimate depends on the assumed source type (double couple, explosion), and the velocity at the source location. This gives an uncertainty of about a factor two in the inferred temporal change in the source location.

Key words: time lapse, volcano monitoring

1 INTRODUCTION

Mount St. Helens began erupting in October 2004 after having been dormant since 1986. The rejuvenated activity has been manifested by a few vent clearing phreatic/phreatomagmatic explosions and subsequent extrusion of a new dacitic lava dome. As of January 2006 this new dome continues to grow in the southern moat between the 1986 dome and the caldera wall. The calculated volume of the extruded dome in the first 9 months of eruption was 60 million m^3 (Schilling *et al.*, 2005).

Since October 2004 extrusion of the viscous lava has often been accompanied by self-similar long-period or hybrid (mixed-frequency) earthquakes, commonly observed at erupting volcanoes. These clones, or families of events, occur as swarms and at times repeat at strikingly regular intervals ranging in duration from 20 seconds to tens of minutes (S. Moran, personal communication). A particularly regular and spectacular set of these events occurred on October 8 through 10, 2004. Although the source process of these events is a subject of debate, most suspect that these events are associated with brittle stick-slip motion of the lava as it is pushed up through the feeding conduit (Harrington *et al.*, 2005; Iverson, 2005).

The highly repeatable nature of these numerous clones suggest similar source mechanisms and source locations occurring in a non-destructive medium. Slight differences in the waveform coda, which appears to evolve gradually over time, are thus likely related to slight variations in source parameters (location and/or mechanism) and/or the media through which elastic waves are propagating.

In this paper we propose that the evolution of seismic codas are a response to variations in Green's function. We analyze a sequence of stacked events occurring during a 24-hour period on Oct. 8, 2004. Each stacked trace is comprised of 15 to 35 traces recorded at vertical component station STD (5 km from the dome) occurring during an hour-long period (Fig. 1). Evolution in waveform coda is evident when comparing stacked traces from throughout the data. Systematic and incremental differences in coda is evident when comparing stacked traces from hour 1 and stacked traces from later ages during the same day (Fig. 2). Here we refer to the

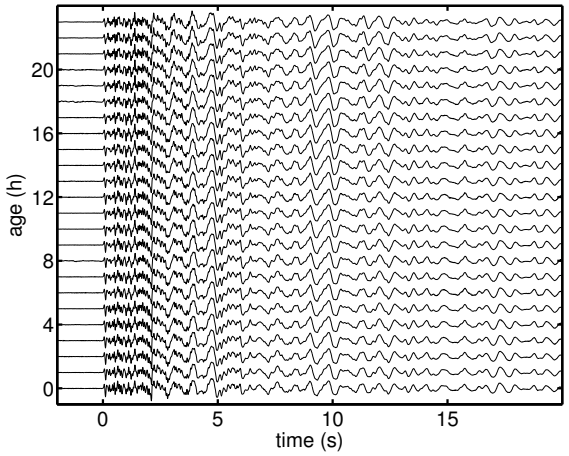

Figure 1. Hourly stacks of the vertical component ground motion recorded at station STD due to repeat events in Mount St. Helens on Oct. 8, 2004. The vertical axis denotes the age, i.e., the lag time relative to the first stacked trace.

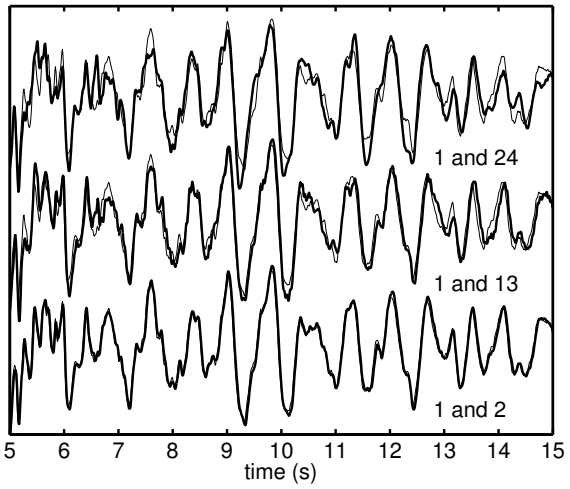

Figure 2. Enlarged superposition of the bottom trace of figure 1 (thin lines), and the waves shown in the 13th and 24th trace of that figure (thick lines).

difference in recording time between traces as *age*, in order to separate it from the *time* within a seismogram.

2 THE REASON FOR THE CHANGE

What causes the change in the waveforms with age? As shown in the example of figure 2, there is no systematic phase shift between trace 1, and traces recorded at later ages. We determined the time shift between trace 1 and later traces by picking the peak of the time-shifted cross-correlation using a moving time window with a length of 2 s. The average time shift is 9 ± 4 ms. This is less than the sampling time. The time shift does not change systematically with age, and it does not change systematically with time. This indicates that the change in the waveforms is not due to a change in velocity.

Does the source-time function change? The recorded waves u are the convolution of the Green's function G and the source-time function S, so that in the frequency domain

$$u(\omega) = G(\omega)S(\omega) \; . \tag{1}$$

This expression also applies to the waveforms that have been time-windowed. The data recorded in a time window for two different ages satisfy

$$\frac{u^{(age1)}_{window1}(\omega)}{u^{(age2)}_{window1}(\omega)} = \frac{G^{(age1)}_{window1}(\omega)}{G^{(age2)}_{window1}(\omega)} \cdot \frac{S^{(age1)}(\omega)}{S^{(age2)}(\omega)} \; , \tag{2}$$

where the subscript indicates the time window applied to the recorded waves and the Green's functions.

Note that we tacitly assume that the windowing does not affect the source-time function. This is the case when the employed window length (5 s) is much larger than the duration of the source-time function. For the weak events that we analyze the source-time function has a typical duration that is much smaller than the used window length.

Suppose that the Green's function does not change with age. In that case expression (2) reduces to

$$\frac{u^{(age1)}_{window1}(\omega)}{u^{(age2)}_{window1}(\omega)} = \frac{S^{(age1)}(\omega)}{S^{(age2)}(\omega)} \; , \tag{3}$$

The same reasoning can be applied to a different time window that does not overlap with the first time window:

$$\frac{u^{(age1)}_{window2}(\omega)}{u^{(age2)}_{window2}(\omega)} = \frac{S^{(age1)}(\omega)}{S^{(age2)}(\omega)} \; , \tag{4}$$

This means that if the Green's function does not depend on age

$$\frac{u^{(age1)}_{window2}(\omega)}{u^{(age2)}_{window2}(\omega)} = \frac{u^{(age1)}_{window1}(\omega)}{u^{(age2)}_{window1}(\omega)} \; , \tag{5}$$

The spectral ratios in this expression correspond, in the time domain, to the deconvolution of the time-windowed data at two different ages.

Figure 3 shows the deconvolution of the waveforms of figure 1 with the first trace. The deconvolved waves are based on the waveforms in window 1 that extends from between 0 and 5 s (thick line), and on the waveforms in window 2 between 5 and 10 s (thin line). Because of attenuation, the spectral content changes with time. We first low-passed filtered the data at 5 Hz, so that the spectral content in both windows is similar. We used a water-level regularization in the deconvolution, i.e., we replaced the spectral ratio $u_1(\omega)/u_2(\omega)$ by $u_1(\omega)u_2^*(\omega)/(|u_2(\omega)|^2 + \varepsilon)$, with ε equal to 1% of the average spectral power. The deconvolved waves are dominated by a peak near $t = 0$ s. This peak reflects the

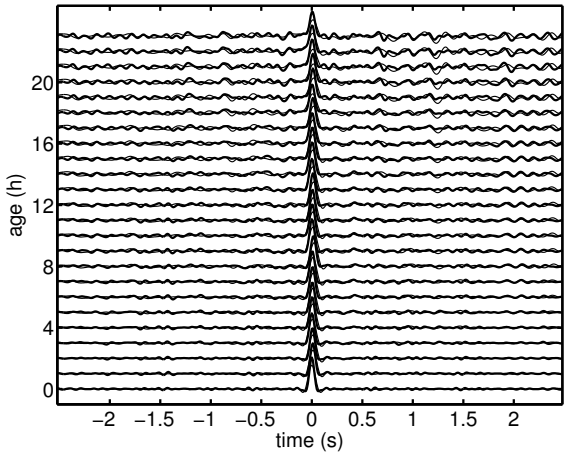

Figure 3. Deconvolution of the waveforms of figure 1 with the wave of the bottom trace (age=0 h). The deconvolution is applied to data low-passed filtered at 5 Hz. The thick line denotes waveforms obtained from a deconvolution of the waves between 0 and 5 s, while the thin line denotes the waveforms time-windowed between 5 and 10 s.

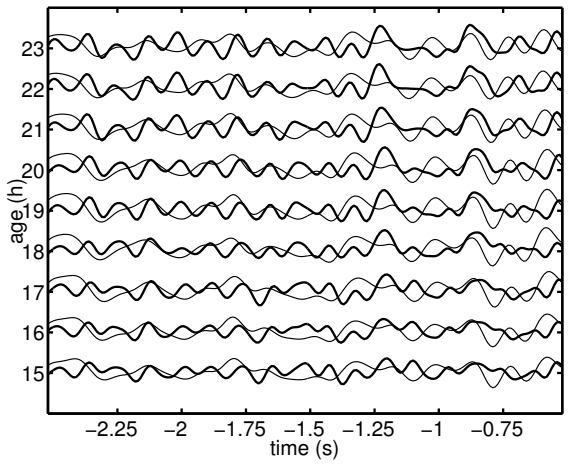

Figure 4. Zoom of the deconvolved waves of figure 3.

similarity of the waveforms recorded at different ages. There are slight variations in the location of this peak that are due to small changes in the origin time of the traces in figure 1; this is an artifact that does not represent systematic variations in source phenomena. The fluctuations in the deconvolved waves in figure 3 grow as a function of age. These fluctuations reflect the changes in the recorded waves with age. Figure 4 shows these fluctuations in detail for later ages. The fluctuations in the deconvolved waves inferred from the data windowed between 0 and 5 s (thick lines) and from the data windowed between 5 and 10 s (thin lines), are uncorrelated. This means that expression (5) does not hold; hence the assumption that the changes in the waveforms are due to changes in the source-time function does not hold. We show in section 3 that the frequency-dependence of the correlation coefficient of time-windowed and bandpass-filtered traces of figure 1 is not compatible with a change in source mechanism.

The Green's function thus changes with age. For a fixed receiver position, the Green's function can change because of two reasons: (i) the medium may change, and/or (ii) the location of the source changes. A change in the wave propagation in the volcano would be reflected in a change in the phase of the arriving waves with age (Roberts *et al.*, 1992; Snieder *et al.*, 2002; Grêt *et al.*, 2006). Since the data do not show a significant phase change with age, we rule out that the wave propagation changes significantly. This leaves the second option, a moving source, as the most likely cause of the changes in the waveforms of figure 1 with age.

In this work we infer the change in the source location with age that explains the changes in the waveforms of figure 1. Our analysis is based on the theory of Snieder and Vrijlandt (2005) who relate the correlation of the coda waves recorded at different ages, to the spatial displacement of the seismic source.

3 THE DECORRELATION OF THE WAVES

As shown in figure 2, the waveforms are highly repeatable, but they do change slowly with age. We quantify this change by computing the correlation coefficient of earliest trace in figure 1 with later traces. Since the correlation coefficient depends, in general, on the employed time window and on frequency, we used various time windows (0-5 s, 5-10 s, 10-15 s, and 15-20 s) and bandpass-filtered the data with a 5th-order Butterworth filter over several frequency bands (2-4 Hz, 4-6 Hz, and 6-10 Hz). Since the data do not show a significant phase shift with age, we did not compute the time-shifted correlation coefficient. Because of attenuation, the signal to noise ratio is poor in the latest time window (15-20 s) for the frequency band with the highest frequencies (6-10 Hz). For this reason we do not include the correlation coefficient in this time window and frequency band in the analysis.

Random noise in the data leads to a bias in the correlation coefficient because it makes the waveforms more dissimilar. One can correct for this bias if the average signal to noise ratio is known (Douma & Snieder, 2006). Under the assumption of stationarity, the statistical properties of the noise do not depend on time, and the noise level can be estimated from the energy in the traces before the first-arrival. In this work we correct for the bias due to random noise by division with a scale factor that is given by the maximum of the correlation coefficient for all nonzero ages. For all employed time windows and frequency bands this maximum is attained for the 4th trace (age = 3 h). The idea behind this scale factor is that for small ages, the waveforms are virtually identical. In that case, the only reason for a reduction

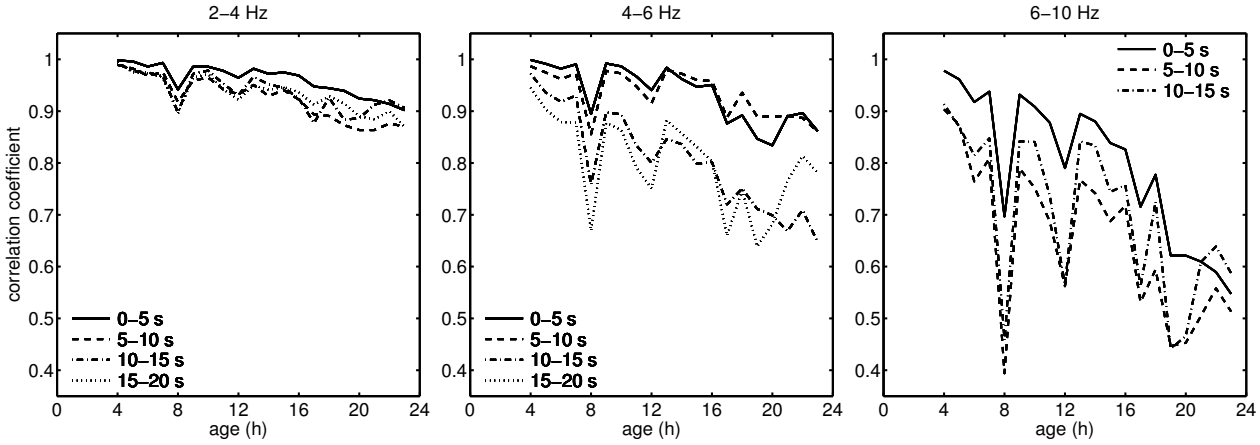

Figure 5. Correlation coefficient between the waveforms of figure 1 with the waveforms at age=0 h, for data band-passed between 2-4 Hz (left panel), 4-6 Hz (middle panel), and 6-10 Hz. The correlation coefficient is computed for time windows from 0-5 s (solid lines), 5-10 s (dashed lines), 10-15 s (dash-dotted lines), and 15-20 s (dotted lines).

of the correlation coefficient from its maximum value $R = 1$ is due to the presence of random noise.

Figure 5 shows the correlation coefficients of the traces of figure 1 computed for various time windows and frequency bands. The correlation coefficient steadily decreases with age. The dip at age = 8 h is due to a noisy trace. The waves at higher frequencies decrease more rapidly with age than do the waveforms at lower frequencies. According to expression (6) of ref. (Snieder & Vrijlandt, 2005), the correlation coefficient is related to the variance of the travel time σ_τ^2 by

$$R = 1 - \frac{1}{2}\overline{\omega^2}\sigma_\tau^2 \,, \tag{6}$$

with $\overline{\omega^2}$ given by

$$\overline{\omega^2} = \frac{\int \dot{u}^2 dt}{\int u^2 dt} \,, \tag{7}$$

where the dot denotes the time derivative. This frequency, and the correlation coefficient, can be directly computed from the data.

The source displacement determines σ_τ. For a given value of σ_τ, expression (6) predicts that higher frequencies give a lower correlation coefficient than lower frequencies do. The correlation coefficients of figure 5 reflect this frequency-dependence of the correlation coefficient. Note that for all frequency bands, the correlation coefficient for the earliest time window (solid lines) is slightly higher than for later time windows. For the later time windows the correlation coefficient does not depend systematically on the center time of the time window. The higher correlation coefficient of the earliest time window can be explained by the difference in the paths taken by the waves arriving in early and later time windows. For later times, the waves take off from the source in all possible directions, and the coda results from the interference of these waves. For early times, the wave preferentially travel along a direct path from the source to the receiver. This implies that the waves recorded in an early time window have a different sensitivity to changes in the source location than the later arriving coda waves do. Since the theory of Snieder and Vrijlandt (2005) is applicable to the coda waves, we do not further analyze the correlation coefficient for the earliest time window (0-5 s).

A change in the source mechanism leads to a change a in the correlation coefficient that is independent of frequency (Robinson *et al.*, 2006). The frequency-dependence of the correlation coefficient shown in figure 5 supports the hypothesis that the changes in the waveform are due to a change in the source position rather than in the source mechanism.

4 THE INFERRED SOURCE DISPLACEMENT

Expressions (6) and (7) relate the data to the variance on the travel-time perturbation through the correlation coefficient R and the squared frequency $\overline{\omega^2}$. Snieder and Vrijlandt (2005) show in their expression (53) that, for a source displacement along the fault, the source displacement and the variance in the travel time are related by

$$\delta_{//fault} = \left[7\left(\frac{2}{v_P^6} + \frac{3}{v_S^6}\right)\Big/\left(\frac{6}{v_P^8} + \frac{7}{v_S^8}\right)\right]^{1/2} \sigma_\tau \,, \tag{8}$$

where v_P and v_S are P- and S-wave velocities, respectively. In this expression σ_τ denotes the variance of the travel time associated with the spatial displacement of the source position averaged over all the waves that leave the source (Snieder & Vrijlandt, 2005; Snieder, 2006). Using expression (6), σ_τ can be retrieved from the correlation coefficient of the waveforms for the unperturbed and perturbed source positions.

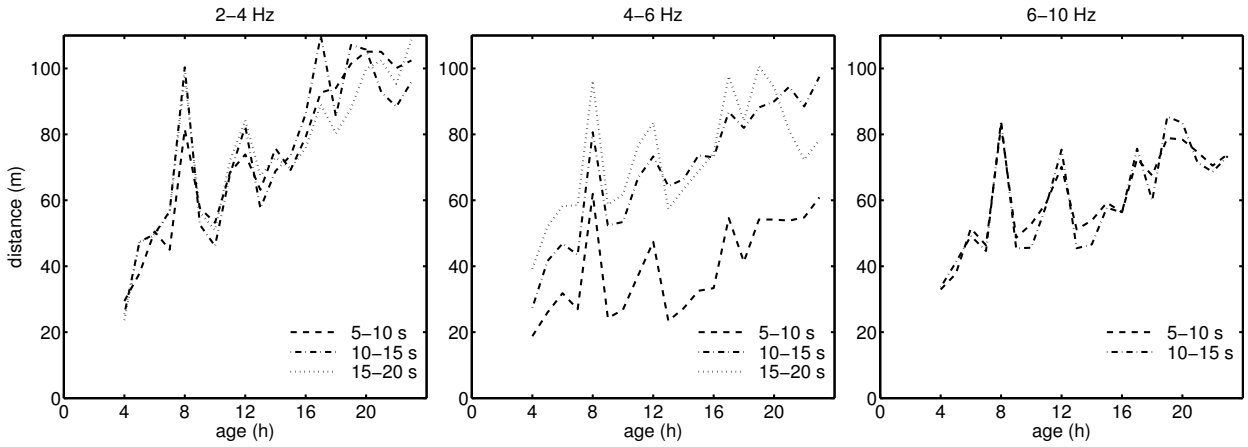

Figure 6. The distance between the event at age=0 h and the event at later times inferred from data band-passed between 2-4 Hz (left panel), 4-6 Hz (middle panel), and 6-10 Hz. The correlation coefficient is computed for time windows from 5-10 s (dashed lines), 10-15 s (dash-dotted lines), and 15-20 s (dotted lines).

Figure 6 shows the source displacement inferred from the correlation coefficients of figure 5, assuming a double-couple source that moves within the fault plane. In this calculation we used $v_S = 2000$ m/s and $v_P = \sqrt{3}v_S$. Note that, apart from the source displacement inferred from the earliest time window (0.5 s), there is a good agreement in the source displacements inferred from the different frequency bands and the different time windows. This agreement provides a consistency check on the assumed model for the change in the waveforms that is based on the assumption that the change in the waveforms is caused by a change in the source position.

The different time windows and frequency band offer redundant estimates of the change in the source location. This redundancy can be used to estimate the uncertainty in the source displacement. Figure 7 shows the average source displacement, and its variance, obtained by averaging the source displacement of figure 6. The source displacement is about 100m/day, and the standard deviation in this estimate is about 10m/day.

The standard deviation in figure 7 does not account for errors that are due to the employed model for the change in the waveforms. The source displacement in figure 7 is based on the assumption that the source moves parallel to the fault plane. This is a natural assumption for aftershocks, but it is not obvious that this is the appropriate model for the events in Mount St. Helens. If the source would be displaced perpendicular to the fault zone, the source displacement follows from the second term of expression (52) of Snieder and Vrijlandt (2005); in that case the source displacement would be 1.33 as large as the source displacement shown in figure 6. If the source would be explosive, expression (49) of Snieder and Vrijlandt (2005) is applicable; this would lead to a source displacement that is 1.72 as large as the source displacement shown in figure 6. Expression (8) is based on body waves only.

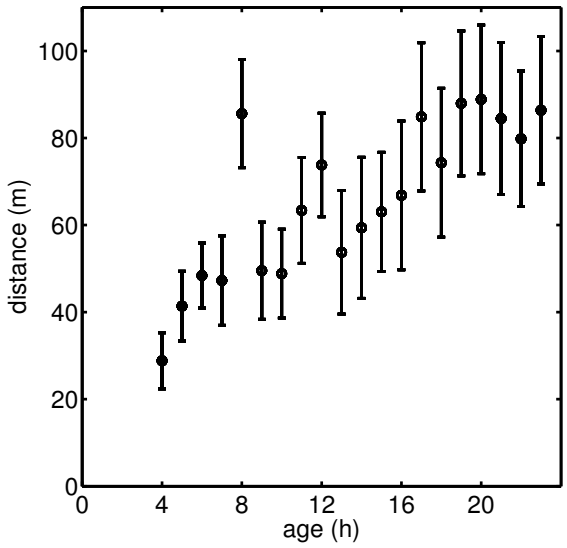

Figure 7. The mean and variance of the event separation as a function of age, computed by averaging the event separation of the different time windows and frequency bands of figure 6.

The lack of precise knowledge in the direction of the source displacement leads to errors in the estimated source displacement that are larger than the standard deviation shown in figure 7. We conclude that the source displacement on this particular day is of the order of 100 m/day, but errors in the assumed model for the source displacement, and errors in the wave velocities near the source, give an error of about a factor of two.

REFERENCES

Douma, H., & Snieder, R. 2006. Correcting for bias due to noise in coda wave interferometry. *Geophys. J. Int.*, **164**, 99–108.

Grêt, A., Snieder, R., & Scales, J. 2006. Time-lapse monitoring of rock properties with coda wave interferometry. *J. Geophys. Res.*, **111**, B03305, doi:10.1029/2004JB003354.

Harrington, R. M., Brodsky, E.E., & Spieler, O. 2005. Slip energy budgets of the Mount St. Helens earthquakes. *EOS Trans. Am. Geophys. Union Fall Meeting*.

Iverson, R.M. 2005. A dynamical model of seismogenic dome extrusion, Mount St. Helens. *EOS Trans. Am. Geophys. Union Fall Meeting*.

Roberts, P.M., Scott Phillips, W., & Fehler, M.C. 1992. Development of the active doublet method for measuring small velocity and attenuation changes in solids. *J. Acoust. Soc. Am.*, **91**, 3291–3302.

Robinson, D., Snieder, R., & Sambridge, M. 2006. Changes in the source mechanism inferred from coda wave interferometry. *in preparation*.

Schilling, S., Denlinger, R., Thompson, R.A., & Messerich, J. 2005. Measuring the dome growth of the 2004-2005 eruption of Mount St. Helens. *EOS Trans. Am. Geophys. Union Fall Meeting*.

Snieder, R. 2006. The theory of coda wave interferometry. *Pure and Appl. Geophys.*, **163**, 455–473.

Snieder, R., & Vrijlandt, M. 2005. Constraining Relative Source Locations with Coda Wave Interferometry: Theory and Application to Earthquake Doublets in the Hayward Fault, California. *J. Geophys. Res.*, **110**, B04301, 10.1029/2004JB003317.

Snieder, R., Grêt, A., Douma, H., & Scales, J. 2002. Coda Wave Interferometry for Estimating Nonlinear Behavior in Seismic Velocity. *Science*, **295**, 2253–2255.